Int. j. adv. multidisc. res. stud. 2026; 6(6):201-206

Received: 13-09-2026
Accepted: 23-10-2026

International Journal of Advanced Multidisciplinary Research and Studies

ISSN: 2583-049X

Three-Dimensional Mapping of Soil Textural Fractions on the Grounds of IFTO, Pedro Afonso Campus, Tocantins, Brazil

[1] Eurides Silva Correia, [2] Helio Lopes Araújo, [3] Elias Mendes Costa, [4] Alexson Filgueiras Dutra, [5] Darley Oliveira Cutrim, [6] Helenilson De Oliveira Francelino, [7] Sergio Nascimento Duarte

[1] Escola Superior de Agricultura "Luiz de Queiroz" ESALQ/USP – Piracicaba – SP, Brazil
[2] Universidade Federal de Rondonópolis – UFR, Rondonópolis – MT, Brazil
[3] Instituto Federal do Tocantins – Araguatins – TO, Brazil
[4] Instituto Federal do Tocantins – Pedro Afonso – TO, Brazil
[5] Instituto Federal do Tocantins – Pedro Afonso – TO, Brazil
[6] Instituto Federal do Tocantins – Pedro Afonso – TO, Brazil
[7] Escola Superior de Agricultura "Luiz de Queiroz" ESALQ/USP – Piracicaba – SP, Brazil

Corresponding Author: **Helio Lopes Araújo**

Abstract

Soil texture, determined by the proportions of sand, silt and clay, is a fundamental indicator of soil physical quality and an important attribute for soil classification. This study mapped the three-dimensional distribution of soil texture in a pasture area at the Instituto Federal do Tocantins (IFTO), Pedro Afonso Campus, Tocantins, Brazil. Forty soil samples were collected at three depth intervals (0–20, 20–40 and 40–60 cm). Spatial modelling combined Ordinary Kriging and the Random Forest machine learning algorithm using environmental covariates derived from a digital elevation model and drone imagery. Clay content increased with depth, from 14% in the surface layer to 22% at 40–60 cm, whereas sand content declined from 71% to 58%, indicating greater textural differentiation in the subsurface. Model performance was generally modest, with R^2 values ranging from -0.04 to 0.21. Ordinary Kriging achieved the highest predictive performance at 40–60 cm (R^2 = 0.21, RMSE = 5.58% and MSE = 4.86%), slightly outperforming Random Forest (R^2 = 0.18, RMSE = 5.72% and MSE = 4.93%). These results indicate that the spatial dependence of the data had a stronger influence on soil texture prediction than the environmental covariates incorporated into the machine learning model. Although predictive accuracy was limited, the integration of geostatistical and geospatial techniques successfully characterised the spatial variability of soil texture. The resulting three-dimensional maps provide valuable information for sustainable soil management, land-use planning and future precision agriculture applications, while establishing a robust baseline for further investigations of soil spatial variability.

Keywords: Soil Texture, Digital Soil Mapping, Geostatistics, Random Forest, Ordinary Kriging

Introduction

Soil texture, defined by the relative proportions of sand, silt and clay, is a fundamental attribute for soil description, identification and classification. This property directly influences soil aggregation, water and air movement, infiltration, water retention and susceptibility to erosion, thereby affecting the performance of agricultural production systems. As a relatively stable property that undergoes little temporal variation, soil texture is one of the principal attributes used in soil characterisation, classification and management. It also provides the basis for understanding a wide range of physical, chemical and biological processes within the soil environment (Augusto *et al*., 2022; Andrade *et al*., 2022) [4, 3].

Particle-size analysis was performed using a combination of physical and chemical dispersion of soil particles. The coarser fractions were separated by sieving, whereas the finer fractions (silt and clay) were determined by sedimentation in accordance with Stokes' law. The particle-size fractions were quantified by gravimetric analysis and the pipette method, which measures the density of the soil suspension. This procedure enables the accurate determination of the particle-size distribution and the relative proportions of the soil fractions within the study area (Almeida *et al*., 2012) [1].

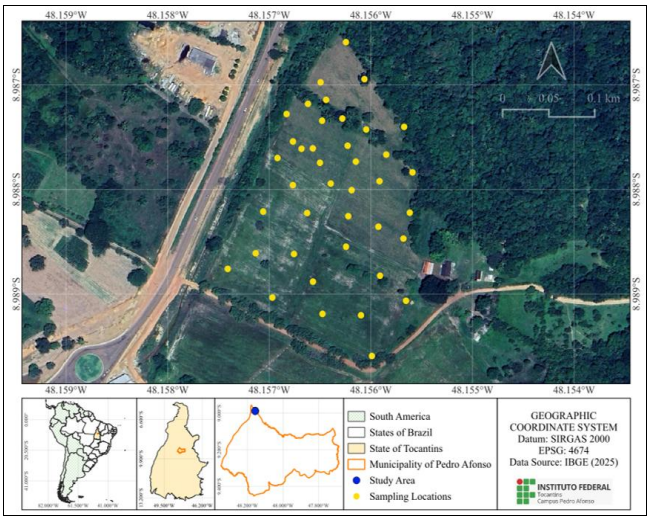
Digital Soil Mapping (DSM) has become a valuable approach for addressing the shortage of detailed soil information, particularly in countries with extensive land areas, such as Brazil (Valadares *et al*., 2024) [27]. DSM integrates soil science, statistics, geographic information systems (GIS) and machine learning to model the spatial and temporal distribution of soil properties. Previous studies have shown that incorporating environmental covariates derived from remote sensing and digital terrain models enhances the predictive performance of mapping models, thereby supporting applications in agricultural planning, sustainable land management and environmental monitoring (Avalos *et al*., 2024; Rosin *et al*., 2023) [5, 18].

Among the most widely employed methods, Ordinary Kriging is recognised as one of the best linear unbiased estimators for the spatial interpolation of soil properties. Its widespread use is largely attributable to its ability to account for the spatial dependence inherent in soil data, thereby providing reliable predictions even under conditions of high spatial variability. The Random Forest algorithm is also extensively applied in Digital Soil Mapping. It is an ensemble machine learning method that combines multiple regression or classification trees to produce robust and accurate predictions. Model performance is internally assessed using out-of-bag validation, while the relative importance of each environmental covariate is simultaneously quantified. This approach enables the production of high-resolution soil texture maps and provides a ranking of predictor variables according to their contribution to model performance (Sahraee *et al*., 2022; Pahlavan-Rad & Akbarimoghaddam, 2018; Dharumarajan & Hegde, 2020) [20, 17, 9].

This study aimed to evaluate the predictive performance of Ordinary Kriging and the Random Forest algorithm for estimating soil texture at depths of 0-20, 20-40 and 40-60 cm, and to generate detailed three-dimensional soil texture maps of the experimental area at the IFTO Pedro Afonso Campus, Tocantins, Brazil.

Material and Methods

The study was conducted in a pasture area located on the experimental farm of the Federal Institute of Tocantins (IFTO), Pedro Afonso Campus, Tocantins, Brazil (Fig 1). According to the Köppen climate classification, the region has a tropical savanna climate (Aw), characterised by a rainy season from November to May and a dry season from June to October, with a mean annual precipitation of approximately 1,700 mm and a mean annual temperature of 29 °C (Silva Neto, 2021; INMET, 2025) [25, 13]. The predominant soil in the experimental area is classified as a Quartzipsamment according to the Brazilian Soil Classification System (Sistema Brasileiro de Classificação de Solos – SiBCS) (Santos *et al*., 2025) [21].



Source: Prepared by the authors

Fig 1: Location of the study area

A total of 40 georeferenced soil samples were collected at three depth intervals (0–20, 20–40 and 40–60 cm). Sampling locations were recorded using a handheld Garmin eTrex 32x GPS receiver (Garmin, 2020) [10].

The soil particle-size distribution (sand, silt and clay) was determined using the pipette method (Teixeira *et al*., 2017) [26]. Sodium hydroxide (NaOH) was used as the chemical dispersing agent, and mechanical agitation was applied to ensure complete particle dispersion. The sand fraction was separated by wet sieving through a 53 µm mesh, whereas the silt and clay fractions were determined by sedimentation according to Stokes' law. All laboratory analyses were conducted at the IFTO Soil Laboratory.

All three particle-size fractions were quantified to provide a comprehensive textural characterisation of the study area. However, spatial modelling was performed only for the sand and clay fractions, as these were considered the most representative indicators of soil textural variability and the most relevant to pedogenetic processes and land management within the study area.

Ordinary Kriging was applied to interpolate the spatial distribution of the soil textural fractions. Semivariogram models were fitted using the R statistical software (R Core Team, 2025) [19], enabling unbiased predictions with minimum estimation variance (Silva *et al*., 1995) [24]. The Random Forest algorithm (Breiman, 2001) [6], also implemented in R, was employed to predict the spatial distribution of soil texture based on environmental covariates, allowing its predictive performance to be compared with that of the geostatistical approach.

The Random Forest model was constructed using an ensemble of regression trees trained on bootstrap samples (Hastie *et al*., 2009) [11]. Model hyperparameters, including

the number of trees and the number of predictor variables randomly selected at each split, were defined according to recommendations reported in the literature (Paiva *et al*., 2020) [16].

The Random Forest model incorporated three groups of predictor variables (Mallah *et al*., 2022) [15]: (i) terrain attributes derived from the digital elevation model (DEM), including slope, aspect, northernness, the Terrain Ruggedness Index (TRI), roughness and the Topographic Position Index (TPI); (ii) spectral indices derived from RGB drone imagery, including the Green Leaf Index (GLI), Triangular Greenness Index (TGI), Soil Colour Index (SCI), and the Red, Green and Blue spectral bands; and (iii) geographic coordinates (latitude and longitude).

The predictive performance of the models developed for mapping the sand and clay fractions was evaluated using Leave-One-Out Cross-Validation (LOO-CV). Model performance was assessed using the coefficient of determination (R^2), the root mean square error (RMSE) and the mean squared error (MSE). To reduce the method-specific bias associated with each interpolation technique and to integrate the complementary spatial information captured by both the geostatistical and machine-learning approaches, the final sand and clay maps were generated using a two-step arithmetic averaging procedure. First, for each soil depth interval (0-20, 20-40 and 40-60 cm), a cell-by-cell arithmetic mean was calculated between the predictions produced by the Random Forest model and those obtained from Ordinary Kriging, using rasters with identical spatial resolution and geographical extent. Arithmetic averaging was adopted as a simple ensemble strategy to produce more stable spatial representations by combining the strengths of both interpolation methods rather than relying on a single modelling technique.

Results and Discussion

Table 1 presents the descriptive statistics for the clay and sand contents at the three sampling depths (0-20, 20-40 and 40-60 cm). Clay content increased with depth, from a mean of 14% in the surface layer to 22% in the deepest layer, whereas sand content exhibited the opposite trend, decreasing from 71% to 58% over the same soil profile. This pattern is likely attributable to the greater vertical translocation of clay particles within the soil profile.

The standard deviation indicated low to moderate variability for both particle-size fractions (clay: 5.96-7.53%; sand: 7.24-8.15%). Clay content exhibited slight positive skewness across all depth intervals, whereas sand content showed negative skewness. This contrasts with the findings of Alves *et al*. (2021) [2] for the Pandeiros River watershed (Minas Gerais, Brazil), where skewness coefficients for the textural fractions were also below 1, indicating distributions that more closely approximated normality.

With respect to kurtosis, clay content exhibited negative values (-0.49 to -0.70), indicating a platykurtic distribution with a lower concentration of observations around the mean. In contrast, sand content displayed a distribution close to normality across most depth intervals, with the exception of the 40-60 cm layer, which showed a slight leptokurtic tendency.

Overall, these results indicate that, although the soil texture data did not follow a perfectly normal distribution, the deviations from normality were relatively small and therefore support the application of both geostatistical and machine learning techniques for the spatial modelling of the analysed particle-size fractions.

Table 1: Descriptive statistics of the soil textural fractions

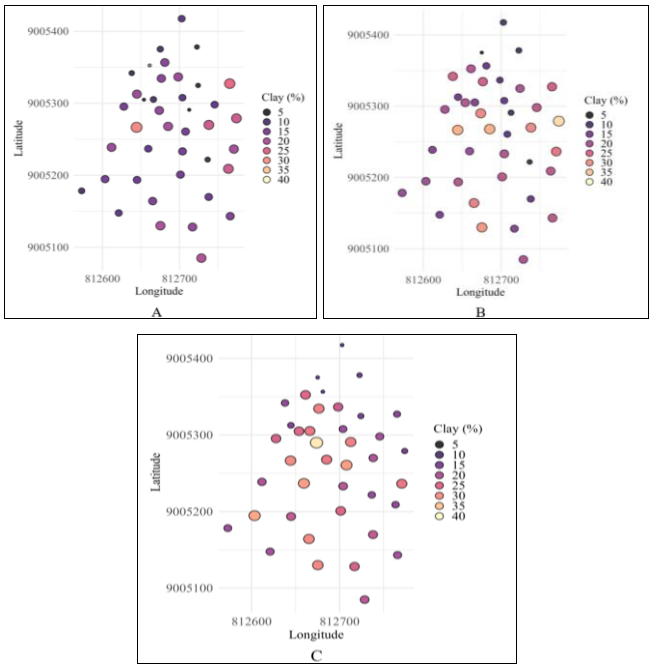
Variable	Depth (cm)	Min. (%)	Mean (%)	Max. (%)	Standard Deviation	Skewness	Kurtosis
Clay	0-20	5	14	29	5.96	0.30	-0.49
	20-40	5	20	37	7.53	0.20	-0.56
	40-60	12	22	38	6.37	0.25	-0.70
Sand	0-20	54	71	82	7.24	-0.65	-0.18
	20-40	44	64	75	7.53	-0.54	-0.43
	40-60	33	58	70	8.15	-0.99	0.76

Distribution of Soil Texture Fractions at Different Depths

Clay Fraction

Fig 2 presents the spatial distribution of clay content at different soil depths, revealing a gradual increase in this fraction with increasing profile depth. The highest clay contents ranged from 25% to 30%, whereas the lowest values varied between 5% and 10%, highlighting the spatial variability of soil texture across the experimental area. This pattern can be attributed to the pedogenetic processes of eluviation and illuviation, which promote the removal of fine particles from the surface layers and their accumulation in subsurface horizons, thereby increasing clay content with depth. Furthermore, landscape position influences sediment redistribution, favouring the deposition of finer particles in areas with lower transport energy.

Similar findings were reported by Coelho (2022) [7], who observed an association between higher clay contents and increased soil organic matter, although the author emphasised that this relationship depends on the pedological characteristics and environmental conditions of each region. In addition, Sauzet *et al*. (2023) [23] demonstrated that eluviation and illuviation are active mechanisms of vertical clay translocation, leading to the enrichment of subsurface horizons and contributing to textural differentiation within soil profiles, thereby supporting the pattern observed in the present study.

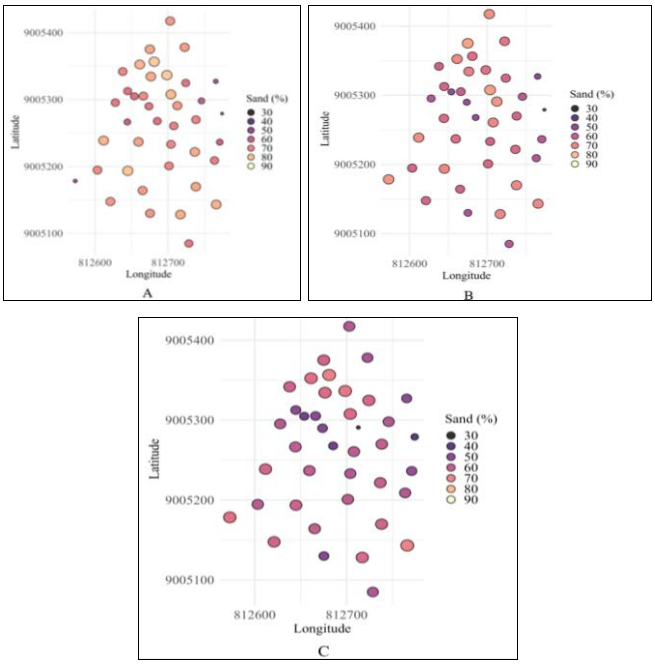


Source: Prepared by the authors

Fig 2: Spatial distribution of clay content at soil depths of 0-20 cm (A), 20-40 cm (B), and 40-60 cm

Sand Fraction

Fig 3 presents the spatial distribution of sand content at different soil depths, showing a pattern opposite to that observed for clay. The highest sand contents were found in the surface layer, reaching values close to 80%, followed by a gradual decrease with depth to approximately 60%. Overall, the distribution was more homogeneous in the surface layer and more heterogeneous in the subsurface layers, reflecting the influence of pedogenetic processes and particle redistribution throughout the soil profile. This pattern corroborates the findings reported by Jena *et al.* (2023) [14], who observed a predominance of sand in the upper soil layers and greater heterogeneity at depth.



Source: Prepared by the authors

Fig 3: Spatial distribution of sand content at soil depths of 0-20 cm (A), 20-40 cm (B), and 40-60 cm

Comparative Analysis of Clay and Sand Distribution Maps

Table 2 presents the performance of the Random Forest and Ordinary Kriging models in estimating clay content at different soil depths, as assessed using Leave-One-Out Cross-Validation (LOO-CV). Overall, both models exhibited limited predictive performance, with coefficients of determination (R^2) ranging from -0.04 to 0.21. The best performance was achieved by Ordinary Kriging at the 40-60 cm depth (R^2 = 0.21), whereas the lowest values were observed in the surface layer (0-20 cm), where the spatial variability of clay content is more strongly influenced by surface processes, including land use and soil management.

Agricultural practices such as ploughing and harrowing disturb the surface soil layer, altering the natural dynamics of pedogenetic processes, including eluviation, illuviation, and clay translocation. In addition, erosional processes contribute to the redistribution of fine particles, increasing the spatial variability of clay content within the surface layer. In contrast, at greater depths, clay distribution is predominantly controlled by more stable structural factors associated with pedogenesis and the parent material.

The RMSE values ranged from 5.58% to 7.10%, whereas the MSE values varied between 4.81% and 5.91%. Although these errors were relatively low in absolute terms, they contrasted with the low coefficients of determination (R^2), reflecting a pattern typically associated with small sample datasets. In such cases, the models produce predictions with physically acceptable error magnitudes but have limited ability to explain the spatial variability of the observed data. Across all evaluated soil depths, Ordinary Kriging performed similarly to, or slightly better than, Random Forest, indicating that the spatial dependence of the data had a greater influence on soil texture prediction than the environmental covariates incorporated into the machine learning model.

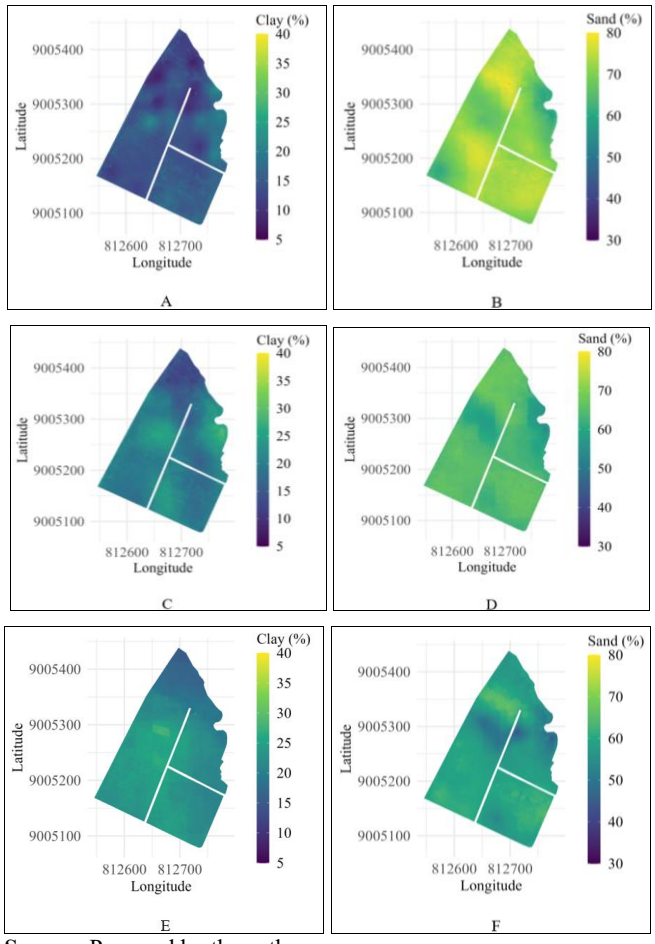
The low R^2 values can be attributed primarily to two factors. First, the limited number of samples compromised both the semivariogram fitting in Ordinary Kriging and the training of the Random Forest model, thereby reducing the statistical robustness of both approaches. Second, the limited environmental and pedological variability within the study area restricted the degree of contrast required for the models to consistently discriminate soil textural classes across space. Consequently, the predictive covariates were only partially able to represent the pedogenetic processes controlling the spatial distribution of particle-size fractions, particularly the influence of the parent material and the illuviation of clay into deeper soil horizons.

Nevertheless, the RMSE and MSE values remained within physically plausible ranges for clay content, suggesting that the identified limitations were primarily associated with the combination of a small sample size and low local spatial variability, rather than with analytical inconsistencies in the original dataset.

Table 2: Performance of the Random Forest (RF) and Ordinary Kriging (OK) models in estimating clay content at different soil depths, as assessed using Leave-One-Out Cross-Validation (LOO-CV)

Model	Depth (cm)	R^2	RMSE (%)	MSE (%)
RF	0-20	0.01	6.25	5.17
RF	20-40	0.09	7.10	5.91
RF	40-60	0.18	5.72	4.93
OK	0-20	-0.04	5.99	4.81
OK	20-40	0.11	7.01	5.89
OK	40-60	0.21	5.58	4.86

Fig 4 presents the mean maps of the clay (A, C, and E) and sand (B, D, and F) fractions, generated from the arithmetic averaging of the estimates obtained at the three evaluated soil depths. These maps provide a comprehensive visualisation of the spatial distribution of soil texture, illustrating the distribution patterns of the two dominant soil particle-size fractions.



Source: Prepared by the authors

Fig 4: Mean maps of clay content: (A) 0-20 cm, (C) 20-40 cm, and (E) 40-60 cm; and sand content: (B) 0-20 cm, (D) 20-40 cm, and (F) 40-60 cm

In the 0-20 cm surface layer, the clay map (A) shows relatively low mean clay contents, ranging from 10% to 25%, with higher concentrations occurring in the eastern part of the study area. In contrast, the sand map (B) displays higher values, ranging from 60% to 80%, particularly along the margins and in the higher-elevation areas. This contrast indicates that the surface soil layer is characterised by a greater proportion of coarse particles, which is in accordance with selective depositional processes and lower aggregate stability.

At the intermediate depth of 20-40 cm, the mean clay map (C) showed a slight increase in clay content, with values ranging from 10% to 30%. Conversely, the sand map (D) revealed a proportional decrease, with mean values ranging from 50% to 70%. This transition suggests a progressive accumulation of fine particles within the subsurface layers, a process commonly associated with the redistribution of materials throughout the soil profile. Demattê *et al*. (2014) [8] observed that, as elevation decreases, soils tend to exhibit finer, more clay-rich textures, reinforcing the influence of topography on the redistribution of soil particle-size fractions, which is consistent with the pattern identified in the present study.

At the 40-60 cm depth, this pattern became even more pronounced. The clay map (E) exhibited the highest mean clay contents, ranging from 15% to 30% across several areas, whereas the sand map (F) showed the lowest mean sand contents observed throughout the soil profile, varying between 40% and 60%. This pattern reinforces the tendency for clay accumulation in deeper soil layers, which is consistent with tropical soil profiles undergoing advanced pedogenetic development. A similar trend was reported by Sartor *et al*. (2025) [22], who observed increased clay activity and cation exchange capacity (CEC) in irrigated soils of the Brazilian semi-arid region, indicating intense mineral transformation and clay mobilisation within the subsurface and deeper soil horizons.

Conclusions

The results demonstrated an increase in clay content and a corresponding decrease in the sand fraction with increasing soil depth, reflecting the natural processes of particle redistribution throughout the soil profile. Although the Random Forest and Ordinary Kriging models exhibited limited predictive performance ($R^2 < 0.25$), the resulting maps adequately represented the spatial patterns of soil texture, indicating higher clay concentrations in lower-elevation areas and a predominance of sand in higher-elevation regions. Among the evaluated methods, Ordinary Kriging achieved the best performance owing to its explicit consideration of the spatial dependence of the data. Overall, digital soil mapping proved to be a valuable approach for characterising the spatial variability of soil texture and supporting soil management and agricultural planning. These findings also highlight the need to improve predictive performance through increased sampling density and the incorporation of additional environmental covariates.

Acknowledgements

The authors would like to acknowledge the Instituto Federal do Tocantins (IFTO) for providing the experimental site and institutional support for this research.

References

1. Almeida BG, Donagemma GK, Ruiz HA, Braida JA, Viana JHM, Reichert JMM, *et al*. Padronização de Métodos para Análise Granulométrica no Brasil, 2012. https://www.researchgate.net/publication/261296999_Padronizacao_de_Metodos_para_Analise_Granulometrica_no_Brasil
2. Alves PFS, Kondo MK, Ferreira VG, Silva RF, Guerra JVS. Variabilidade espacial e análise multivariada dos atributos físicos do solo em uma microbacia do rio

Pandeiros. Geo Uerj. 2021; 39:e40190-e40190. Doi: https://doiorg/1012957/geouerj
3. Andrade R, Mancini M, Teixeira AFS, Silva SHG, Weindorf DC, Chakraborty S, *et al*. Proximal sensor data fusion and auxiliary information for tropical soil property prediction: Soil texture Geoderma. 2022; 422:115936. Doi: https://doiorg/101016/JGEODERMA2022115936
4. Augusto MVS, Demetrio GB, Lajus CR, Azevedo-Ribeiro PF, Reis Duarte E, Sauer AV. Preservação de recursos naturais através de práticas de manejo e seus impactos na qualidade física do solo Uniciências. 2022; 26(2):108-119. Doi: https://doiorg/1017921/1415-51412022v26n2p108-119
5. Avalos FAP, Menezes MD, Acerbi Júnior FW, Curi N, Avanzi JC, Silva MLN. Evaluation of Synthetic-Temporal Imagery as an Environmental Covariate for Digital Soil Mapping: A Case Study in Soils under Tropical Pastures Resources. 2024; 13(2):32. Doi: https://doiorg/103390/RESOURCES13020032
6. Breiman L. Random Forests Machine Learning, 2001, 5-32. Doi: https://doiorg/101023/A:1010933404324
7. Coelho JM. Variabilidade espacial de atributos de um latossolo vermelho em diferentes profundidades sob o cultivo de cana-de-açúcar, 2022. http://hdlhandlenet/11449/243315
8. Demattê JA, Alves MR, Gallo BC, Fongaro CT. Detecção de limites de solos por dados espectrais e de relevo Revista Brasileira de Ciência do Solo. 2014; 38:718-729. Doi: https://doiorg/101590/S0100-06832014000300004
9. Dharumarajan S, Hegde R. Digital mapping of soil texture classes using Random Forest classification algorithm Soil Use and Management. 2020; 38:135-149. Doi: https://doiorg/101111/sum12668
10. Garmin. ETREX® 22X/32X Manual doproprietário, 2020. https://www8garmincom/manuals/webhelp/eTrex22x-32x/PT-BR/eTrex_22x_32x_OM_PT-BRpdf
11. Hastie T, Tibshirani R, Friedman J. The Elements of Statistical Learning. Springer New York, 2009. Doi: https://doiorg/101007/978-0-387-84858-7
12. IBGE - Instituto Brasileiro de Geografia e Estatística, 2025. https://wwwibgegovbr/geociencias/organizacao-do-territorio/malhas-territoriais/15774-malhashtml
13. INMET - Instituto Nacional de Meteorologia. Estação: Pedro Afonso A020, 2025. Available at: <https://tempoinmetgovbr/TabelaEstacoes/A020> Acesso em: 28 maio
14. Jena RK, Moharana PC, Dharumarajan S, Sharma GK, Ray P, Deb Roy P, *et al*. Spatial prediction of soil particle-size fractions using digital soil mapping in the North Eastern Region of India. Land. 2023; 12(7):p. 1295. Doi: https://doiorg/103390/land12071295
15. Mallah S, Delsouz Khaki B, Davatgar N, Scholten T, Amirian-Chakan A, Emadi M, *et al*. Predicting Soil Textural Classes Using Random Forest Models: Learning from Imbalanced Dataset. Agronomy. 2022; 12(11):2613. Doi: https://doiorg/103390/AGRONOMY12112613
16. Paiva R, Oliveira S, Martins W, Parente L. Análise de metacaracterísticas para classificação de uso e cobertura do solo utilizando random forest In: Workshop de Computação Aplicada à Gestão do Meio Ambiente e Recursos Naturais (WCAMA). SBC, 2020, 71-80. Doi: https://doiorg/105753/wcama202011021
17. Pahlavan-Rad MR, Akbarimoghaddam A. Spatial variability of soil texture fractions and pH in a flood plain (case study from eastern Iran). Catena. 2018; 160:275-281. Doi: https://doiorg/101016/jcatena201710002
18. Rosin NA, Demattê JAM, Poppiel RR, Silvero NEQ, Rodriguez-Albarracin HS, Rosas JTF, *et al*. Mapping Brazilian soil mineralogy using proximal and remote sensing data. Geoderma. 2023; 432:116413. Doi: https://doiorg/101016/JGEODERMA2023116413
19. R Core Team R. A Language and Environment for Statistical Computing. R Foundation for Statistical Computing, 2025.
20. Sahraee N, Landi A, Hojati S. Digital mapping of soil texture components in part of Khuzestan plain lands using machine learning models. Iranian Journal of Soil and Water Research. 2022; 53(10):2261-2276. Doi: https://doiorg/1022059/IJSWR2022348442669360
21. Santos HG, Jacomine PKT, Anjos LHC, Oliveira VA, Lumbreras JF, Coelho MR, *et al*. Sistema Brasileiro de Classificação de Solos 6a edição revista e ampliada. Brasília DF: Embrapa, 2025. http://wwwinfotecacnptiaembrapabr/handle/doc/1176834
22. Sartor LR, Ruiz F, Costa PA, Oliveira DP, Romero RE, Souza Júnior VS, *et al*. Irrigation reshapes weathering and pedogenesis in calcareous soils of tropical dryland (NE Brazil). Catena. 2025; 255:p.109040. Doi: https://doiorg/101016/jcatena2025109040
23. Sauzet O, Cammas C, Gilliot JM, Montagne D. Long-term quantification of the intensity of clay-sized particles transfers due to earthworm bioturbation and eluviation/illuviation in a cultivated Luvisol. Geoderma. 2023; 429:116251. Doi: https://doiorg/101016/JGEODERMA2022116251
24. Silva EF, Hissa H, Macedo JR, Oliveira MT, Capeche C. Metodologia para geração de mapas de fertilidade do solo utilizando o interpolador de krigagem, 1995. https://wwwalicecnptiaembrapabr/alice/handle/doc/331652
25. Silva Neto VL, Souza LBE, Viola MR, Morais MAV. Variabilidade espacial e temporal da precipitação no Estado do Tocantins Brasil. Research Society and Development. 2021; 10(3):e44310313545. Doi: https://doiorg/1033448/RSD-V10I313545
26. Teixeira PC, Donagemma GK, Fontana A, Teixeira WG. Manual de métodos de análise de solo 3 ed. ver. e ampl. Brasília DF: Embrapa, 2017. https://wwwembrapabr
27. Valadares AP, Coelho RM, Gamba CTC. Mapeamento pedológico digital com base em objetos a partir de unidades elementares de relevo. Revista do Departamento de Geografia. 2024; 44:e176980-e176980. https://doiorg/1011606/EISSN2236-2878RDG2024176980